Discrimination of form in images corrupted by speckle

Vijaya N. Korwar and John R. Pierce

The problem investigated is that of a human observer having to distinguish between certain specified geometrical forms corrupted by speckle—an idealization of the problem of a scientist studying a synthetic aperture radar map. Specifically, the cases of two simple alternative forms and of two and four orientations of a simple form have been considered. A theoretical model is developed for the observer's decision process by analogy with optimal receiver theory, and the probability of a correct decision is related to form parameters like size, contrast, and looks. These calculations are verified by psychophysical experiments using computer-simulated pictures.

I. Introduction

The phenomenon of speckle[1–3] in coherent systems and the degradation of picture quality caused by speckle[4–6] have long been known. The work described here was motivated by the problem of picture degradation by speckle in synthetic aperture radar (SAR) systems,[7–9] which are coherent high-resolution radar systems used for terrain mapping; however, the results are applicable to other systems where speckle obscures desired detail in pictures. In particular, recent and proposed SAR systems, such as those in the JPL missions SEASAT, VOIR, SIR-A, will provide oceanographers and geologists with land and ocean maps. In all these cases, the pictures are viewed by a human observer who often tries to identify forms in the picture. Usually, the identification problem can be thought of as one in which the observer has various possible alternatives in mind, and he believes some feature he has detected in the picture to be one of these alternative forms. In this paper, we consider some simple cases of this idealized form identification problem.

In another paper,[10] we have considered the problem of detecting a feature in a speckled background; here we assume that the feature has already been detected and focus on the internal structure of the feature rather than on the whole picture. For this reason, we neglect the effect of the background by assuming that the form to be identified is set in a completely dark background.

Specifically, we consider three cases of discrimination, i.e., discriminating between two possible forms, two possible orientations of a given form, and four possible orientations of a given form. Our aim here is to try to relate the parameters of the possible alternatives to their distinguishability. To make theoretical calculations, we have chosen simple geometrical forms. However, the techniques used here can be used for more complex forms as well. We use techniques analogous to those for the optimal reception of signals in noise.[11] This kind of technique has previously been applied by Bernard[12] to the problem of discriminating forms in additive white Gaussian noise, which is even closer to the communications problem mentioned above.

We verify our predictions with simulated pictures and psychophysical experiments.

II. Picture Parameters

It is well known that speckle effects decrease with an increase in the number of looks L, i.e., the number of independent estimates of each pixel intensity that are averaged together to form a pixel in the final picture. These looks are obtained in SAR systems by various techniques such as the use of different carrier frequencies, aspect angles, or polarizations. Each of these techniques increases the complexity of a digital SAR processor required to achieve a given resolution cell size.

We will specifically consider forms that, in the absence of speckle, can be described by two levels of intensity. We denote the fractional difference in intensity of these two levels by b. Thus we can denote the two levels by $P_0(1 + b)$ and P_0. We will refer to these two levels as the bright and dark levels, respectively.

Both authors are with California Institute of Technology, Pasadena; V. N. Korwar is in the Jet Propulsion Laboratory, California 91103, and J. R. Pierce is in the Electrical Engineering Department, California 91125.

Received 24 June 1980.
0003-6935/81/020320-06$00.50/0.

Experiments showed that the absolute intensity P_0 does not noticeably influence form discriminability, provided the brightness corresponding to P_0 lies well within the range of brightness sensitivity of the observer's visual system. Hence P_0 will not figure in our results and is only defined for the sake of generality of analysis. However, it is clear that increasing the contrast ratio $(1 + b)$ between bright and dark portions of a form should increase its distinctiveness and hence its discriminability with respect to another form. To see why $(1 + b)$ is important, consider the processing of raw SAR data to produce an image. This involves a 2-D matched filtering of the signal return,[7] and the autocorrelation function of the filter impulse response is not, in practice, the ideal δ function. An increase in the integrated side-lobe ratio (ISLR) of this impulse response reduces the contrast between a feature and its surroundings. Reducing the ISLR while meeting other SAR specifications requires careful system design.

These considerations show the desirability of performing a trade off between L and $(1 + b)$ required to achieve a desired level of form recognizability.

Other parameters that can affect the discriminability of a set of forms are the size and shape of the forms. Each form that we will consider is derived from a $D \times D$ square (where we will always specify size in pixels) consisting of nine smaller squares, each of size $J \times J$, with $D = 3J$. One or two of these nine smaller squares are dark, while the others are all bright. The forms are shown in Figs. 1 and 2. The cases of Figs. 1(a) and (b) will be treated identically as explained below. The distinction between the cases of Figs. 1 and 2 is that, in Fig. 1, the possible alternatives differ in shape, while in Fig. 2, they are merely different orientations of the same form.

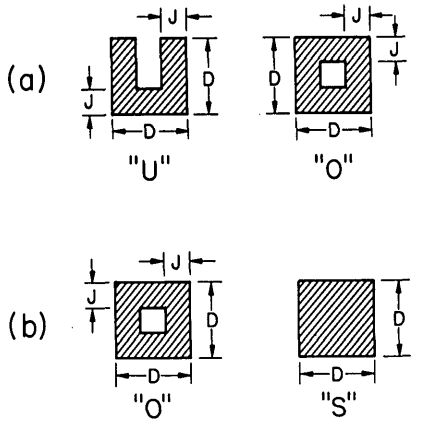

Fig. 1. Forms used in two alternative forms experiments: (a) set 1: U vs O; (b) set 2: O vs S.

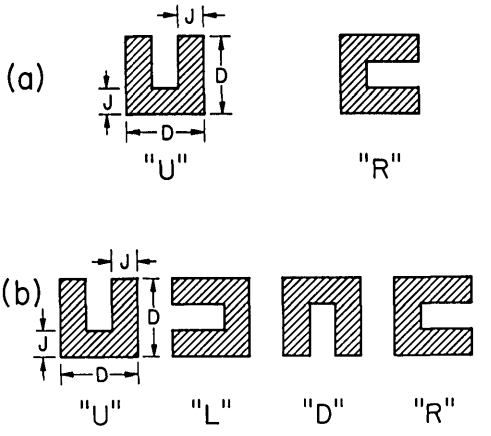

Fig. 2. Forms used in (a) two alternative orientations experiments = set 3; (b) four alternative orientations experiments = set 4.

III. Discrimination Model

Our discrimination model for the observer's eye–brain combination is based on the following assumptions:

(a) Previous work has demonstrated,[13] as one would expect, that two forms become more easily discriminable as the difference between them increases. To characterize this difference, we assume that each form can be represented in terms of nine orthogonal spatial components, each component representing the total power reflected by the J^2 pixels of one of the nine squares of size $J \times J$. The justification for neglecting the fine structure within each of these nine squares is that the observer is told exactly what the forms are, so that his brain will examine the nine squares of size J^2 as nine units. The observer gets an idea of how large the $J \times J$ squares are by examining a low-noise version of the same forms before making decisions on a test case. This method also provides an equivalent of a training period for the observer.[14]

We then assume that the observer's visual system performs a spatial summation over each of the J^2 pixels in every unit of the form. This assumption of summation is supported by previous work provided the $J \times J$ squares subtend less than ~10 min of arc at the eye.[15–18]

(b) In the case of Fig. 1(a) or (b), we assume that the observer looks at a particular component that we call C and decides if it is bright or dark. In Fig. 1(b), this component C is the central square of the form; in Fig. 1(a) it is the central one in the top row. We assume that the observer derives his standard of bright and dark from the squares that he knows to be bright or dark and from his knowledge of $(1 + b)$.

In the case of Figs. 2(a) and (b), there is no need for an absolute judgment of bright or dark; the observer merely has to decide which of two or four relevant components is the darkest. In all cases, he behaves as an optimal maximum likelihood detector would.[11]

Further justification for this model is given elsewhere.[19]

IV. Theoretical Calculations

A. Case of Two Alternatives of Fig. 1(a) or (b)

Although the two shapes may be characterized by nine orthogonal components, they differ only in one of components C so that, to calculate the probability p_c of correct decision, only this component C need be considered. This component C can be either P_0M or P_0 $(1 + b)M$, where $M = LJ^2$ if perfect integration over all the

Table I. Two Alternative Forms; Set 1 (*U* and *O*)

$(1+b)$ dB	L	J	$M =$ (a) LJ (b) LJ^2	No. of samples	Probabilities: Theoretical p_c	Probabilities: Experimental $\hat{p}_c$	Bounds on $\hat{p}_c$ Lower, Upper
1	6	5	30	81	0.76	0.78	0.67, 0.86
			150		0.92		
	15	3	45	256	0.78	0.69	0.63, 0.75
			135		0.91		
	8	6	48	64	0.79	0.91	0.81, 0.97
			288		0.98		
	7	7	49	49	0.79	0.86	0.73, 0.94
			243		0.96		
	10	5	50	81	0.79	0.85	0.75, 0.92
			250		0.97		
	17	3	51	256	0.79	0.86	0.81, 0.90
			153		0.92		
	20	3	60	256	0.82	0.78	0.72, 0.83
			180		0.94		
	13	4	52	144	0.79	0.82	0.75, 0.88
			208		0.95		
	20	5	100	81	0.87	0.91	0.82, 0.96
			500		0.99		
	34	3	102	356	0.88	0.83	0.79, 0.87
			306		0.98		
3	1	5	5	100	0.78	0.85	0.76, 0.91
			25		0.96		
	2	3	6	256	0.80	0.88	0.83, 0.92
			18		0.93		
	8	3	24	256	0.95	0.98	0.96, 1.0
			72		0.998		
	6	4	24	144	0.95	0.98	0.94, 1.0
			96		0.999		
	5	5	25	81	0.95	1.0	0.96, 1.0
			125		0.999		
	34	3	102	100	0.999	1.0	0.96, 1.0
			306		$1-10^{-6}$		
5	1	1	1	160	0.70	0.67	0.59, 0.74
			1		0.70		
	1	2	2	192	0.78	0.78	0.71, 0.84
			4		0.87		

Table II. Two Alternative Forms; Set 2 (*O* and *S*)

$(1+b)$ dB	L	J	$M =$ (a) LJ (b) LJ^2	No. of samples	Probabilities: Theoretical p_c	Probabilities: Experimental $\hat{p}_c$	Bounds on $\hat{p}_c$ Lower, Upper
1	6	5	30	100	0.76	0.84	0.75, 0.91
			150		0.92		
	10	5	50	100	0.79	0.80	0.71, 0.87
			250		0.97		
	17	3	51	256	0.79	0.82	0.77, 0.86
			153		0.92		
	20	5	100	100	0.87	0.92	0.85, 0.97
			500		0.99		

pixels in the $J \times J$ squares is performed by the observer's eye. We also consider the case $M = LJ$ to account for some suboptimal combination of the J^2 squares. The probability density functions (pdfs) of the component C, when C is dark or bright, are given,[20] respectively, by

$$p_d(x) = \frac{1}{P_0^M} x^{(M-1)} \frac{\exp(-x/P_0)}{\Gamma(M)} \quad (\text{for } x > 0), \tag{1}$$

$$p_b(x) = \frac{1}{P_0^M (1+b)^M} x^{(M-1)} \frac{\exp\{-x/[P_0(1+b)]\}}{\Gamma(M)} \quad (\text{for } x > 0), \tag{2}$$

with both pdfs zero if $x < 0$.

The intersection of these two pdf curves gives us a threshold intensity x_t, above which the brighter alternative is chosen and below which the darker one is chosen. By direct calculation, we find

$$x_t = P_0 [M \ln(1+b)] \left(\frac{1+b}{b}\right). \tag{3}$$

The probability of error given that the brighter alternative is actually present is

$$p(e|b) = \int_0^{x_t} p_b(x) dx, \tag{4}$$

and similarly the probability of error given the darker alternative is

Table III. Two Orientations; Set 3 (*U* and *R*)

(1 + *b*) dB	*L*	*J*	*M* = (a) *LJ* (b) LJ^2	No. of samples	Probabilities Theoretical p_c	Probabilities Experimental $\hat{p}_c$	Bounds on $\hat{p}_c$ Lower, Upper
1	6	5	30	100	0.81	0.85	0.76, 0.91
			150		0.977		
	10	5	50	100	0.87	0.96	0.90, 0.99
			250		0.995		
	17	3	51	256	0.88	0.86	0.81, 0.90
			153		0.98		
	13	4	52	144	0.88	0.87	0.80, 0.92
			208		0.99		
	20	5	100	100	0.95	1.0	0.96, 1.0
			500		0.9998		

$$p(e|d) = \int_{x_t}^{\infty} p_d(x)dx. \tag{5}$$

The probability of correct decision is then, for equally likely forms,

$$p_c = 1 - \tfrac{1}{2}[p(e|d) + p(e|b)]. \tag{6}$$

In Fig. 1(a), the brighter alternative corresponds to form O, while in Fig. 1(b), the brighter alternative corresponds to form S.

The value of p_c can be calculated from the above equations using either computer integration or γ distribution tables. Since the usual γ distribution tables are not extensive enough for our purposes, we used numerical integration. For large M, we can use the Gaussian approximations for the pdfs involved and then use normal distribution tables that are quite extensive. For $M \geq 25$, we found by direct evaluation that the Gaussian approximation gave errors of less than ± 0.02, so this is the technique we use for $M \geq 25$. Tables I and II give theoretical and experimental results. The bounds shown on the experimental results are 95% confidence intervals obtained by the standard statistical methods[21] for estimating percentages.

The use of the Gaussian approximation, along with a further approximation for $b \ll 1$, leads to the following useful quick approximation to the values of the threshold level x_t and p_c:

$$x_t \simeq P_0 M[1 + (b/2)], \tag{7}$$

$$p_c \simeq 1 - \tfrac{1}{2}\left\{Q\left(\frac{b\sqrt{M}}{2(1+b)}\right) + Q\left(\frac{b\sqrt{M}}{2}\right)\right\}, \tag{8}$$

where

$$Q(x) = \frac{1}{\sqrt{2\pi}} \int_x^{\infty} \exp(-z^2/2)dz \tag{9}$$

is the usual $Q(\cdot)$ function.

These results are very similar to the ones obtained for an optimal receiver for two binary antipodal signals.[11]

B. Case of Two Orientations [Fig. 2(a)]

Here the observer has to decide which of two components C_1 or C_2 is brighter. In Fig. 2(a), C_1 and C_2 are for the top central square and the right central square. We can see that

$$p_c = \int_0^{\infty} p_b(x)dx \int_0^{x} p_d(y)dy, \tag{10}$$

with $p_b(x)$, $p_d(x)$ as before. By numerical evaluation we can obtain p_c. For $M > 25$, we can use the Gaussian approximation for $p_b(x)$ and $p_d(x)$ and obtain the approximation

$$p_c \simeq 1 - Q\left\{\frac{b\sqrt{M}}{\sqrt{2}[1 + (1+b)^2]}\right\}. \tag{11}$$

We find agreement to within ± 0.02 using this equation for all $M > 25$. The experimental and calculated results are shown in Table III.

Equation (11) resembles what would be obtained for the optimal detection of two orthogonal signals[11] in noise, and therefore the p_c for given b and M is a little higher in this case than in the case of the Fig. 1 forms, which resemble binary antipodal signals.

C. Case of Four Orientations [Fig. 2(b)]

In this case, the observer decides which of four basis squares (top center, bottom center, left center, or right center) is darkest. The probability of correct decision is

$$p_c = \int_0^{\infty} p_d(x)\left[\int_x^{\infty} p_b(y)dy\right]^3 dx. \tag{12}$$

These p_c were numerically evaluated for various b, L, J, and the results are shown in Table IV along with the experimental results.

In all cases, the results were calculated assuming both $M = LJ$ and $M = JL^2$.

V. Simulations and Experiments

Computer-simulated speckled patterns that were equally likely to be one of the allowable alternative forms were photographed using an on-line image generator (Dichomed). Each pixel of the speckle-corrupted picture was generated by averaging the squares of $2L$ independent, identically distributed Gaussian pseudorandom variables with variances proportional to the intensity P_0 or $P_0(1 + b)$ of the corresponding unspeckled pixel. The justification for this technique is given by Guenther *et al.*,[22] who use it in simulating fully developed speckle passed through a linear filter whose transfer function represents temporal averaging.

Each picture simulated had a large number of patterns of fixed b, L, J values. The patterns were then shown to the observer one at a time through a hole in a black mask, and he had to decide between the specified

Table IV. Four Orientations; Set 4 (*U, D, L, R*)

(1 + *b*) dB	*L*	*J*	*M* = (a) *LJ* (b) LJ^2	No. of samples	Probabilities: Theoretical p_c	Probabilities: Experimental $\hat{p}_c$	Bounds on $\hat{p}_c$ Lower, Upper
1	6	5	30	100	0.62	0.70	0.60, 0.79
			153		0.94		
	10	5	50	100	0.73	0.82	0.73, 0.89
			250		0.99		
	17	3	51	256	0.73	0.82	0.77, 0.86
			153		0.95		
	13	4	52	144	0.73	0.81	0.74, 0.87
			208		0.97		
	20	5	100	100	0.88	0.95	0.89, 0.99
			500		0.999		

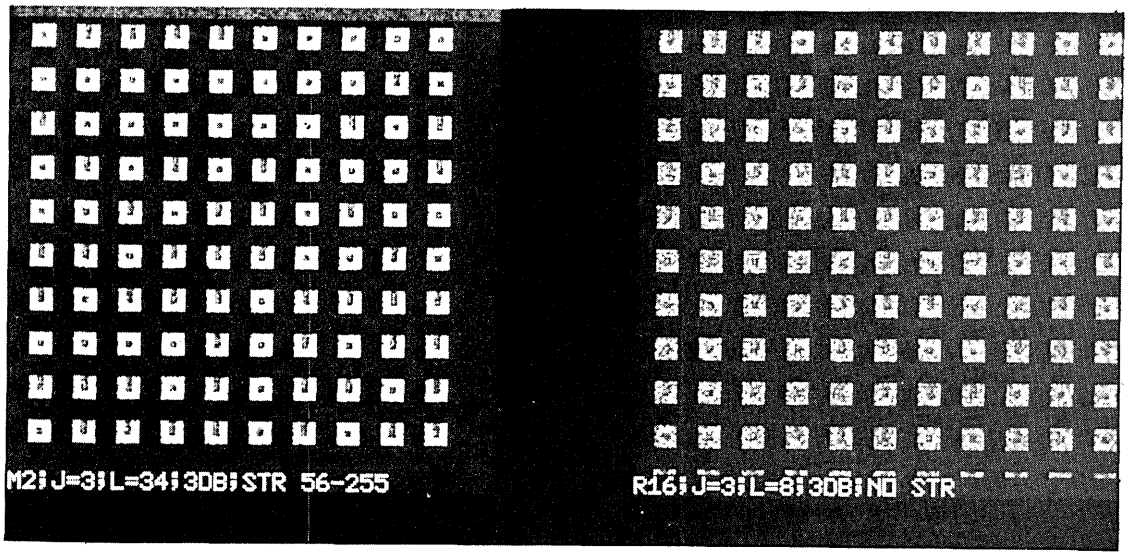

Fig. 3. Examples of simulated pictures. Both photographs have $J = 3$ and 3-dB contrast: (left) $L = 34$; (right) $L = 8$.

alternatives. Before each change of J and b, he was shown unspeckled versions of the forms allowed, which he was told were equally likely (as they were).

The experimental probability of correct decision $\hat{p}_c$ was estimated by the fraction of correct responses made by the observer. These are shown in Tables I–IV along with the theoretical results.

Figure 3 shows some examples of the simulated pictures and demonstrates the improvement in discriminability with looks. In both pictures shown in Fig. 3, we have $J = 3$, $b = 1$, but the picture with $L = 34$ has much more identifiable forms than the one with $L = 8$.

VI. Results

We find from our theory and experiments that (a) the $\hat{p}_c$ values obtained experimentally are almost always between the values calculated theoretically for the two cases $M = LJ$ and $M = LJ^2$; (b) the use of the Gaussian approximation leads to simple expressions for p_c, which are, for large M, very close to the values obtained using the exact γ distribution and numerical integration.

VII. Extension to Other Forms

Theoretically, any set of alternative forms can be represented approximately by a finite set of orthogonal components, using the model given here, and p_c can be represented as an integral. As the number of intensity levels allowed in the unspeckled forms increases from the value of 2 assumed here, we have a problem analogous to that of multilevel, as opposed to binary, quantization in communications,[11] which makes p_c harder to calculate. Also, of course, as the number of orthogonal components increases and the alternatives differ in more components, the integral for p_c becomes harder to evaluate. However, the model, at any rate, is expected to be useful for forms of reasonable complexity other than the ones used here.

VIII. Conclusions

We have demonstrated that the model that we have assumed for discrimination gives results that agree with experiment for a wide range of parameters. The model can be applied to more complex forms than the ones considered here.

We may compare the relative difficulties involved in detecting a feature and identifying its shape as follows: We have shown elsewhere[10,19] that, to detect a $D \times D$ square in a 100×100, 12-look, 1-dB picture with 95% certainty, we need a D of ~ 7. To be able to discriminate between two alternative forms as in Fig. 1(a) in a 12-look 1-dB picture with 95% certainty, we know from Table I that we need $J = 4$ or $D = 12$ even by the optimistic estimate that uses $M = LJ^2$.

This gives an idea of how much more stringent the system requirements are to obtain a system that gives tolerable form discrimination as opposed to one that merely provides feature detectability.

We would like to thank various members of the Jet Propulsion Laboratory, in particular, E. C. Posner and Chialin Wu for helpful discussions and R. G. Piereson for financial support and use of the facilities used in the simulations.

This work was carried out in part at the Jet Propulsion Laboratory, California Institute of Technology, Pasadena, under contract NAS7-100, sponsored by the National Aeronautics and Space Administration.

References

1. J. D. Rigden and E. I. Gordon, Proc. IRE **50,** 2367 (1962).
2. J. W. Goodman, J. Opt. Soc. Am. **66,** 1145 (1976).
3. J. C. Dainty, Ed., *Laser Speckle and Related Phenomena* (Springer, Berlin, 1975).
4. J. C. Dainty, Opt. Acta **18,** 327 (1971).
5. N. George, J. S. Bennett, B. D. Guenther, and C. R. Christensen, J. Opt. Soc. Am. **66,** 1282 (1976).
6. A. Kozma and C. R. Christensen, J. Opt. Soc. Am. **66,** 1257 (1976).
7. R. D. Harger, *Synthetic Aperture Radar Systems: Theory and Design* (Academic, New York, 1970).
8. W. M. Brown, IEEE Trans. Aerosp. Electron. Syst. **AES-3,** 217 (1976).
9. L. J. Porcello, N. G. Massey, R. B. Innes, and J. M. Marks, J. Opt. Soc. Am. **66,** 1305 (1976).
10. V. N. Korwar and J. R. Pierce, Appl. Opt. **20,** 312 (1981).
11. J. M. Wozencraft and I. M. Jacobs, *Principles of Communication Engineering* (Wiley, New York, 1965).
12. T. W. Bernard, *A Symposium on Sampled Images* (Perkin-Elmer, Norwalk, Conn., 1971).
13. J. W. Wulfech and J. H. Taylor, Eds., *Form Discrimination as Related to Military Problems,* Publication 561, NAS-NRC (U.S. GPO, Washington, D.C., 1957).
14. D. M. Green and J. A. Swets, *Signal Detection Theory and Psychophysics* (Wiley, New York, 1966).
15. T. N. Cornsweet, *Visual Perception* (Academic, New York, 1970).
16. F. Radcliff, M. K. Hartline, and W. H. Miller, J. Opt. Soc. Am. **53,** 110 (1963).
17. H. Helson, J. Opt. Soc. Am. **53,** 179 (1963).
18. L. D. Harmon and B. Julesz, Science **180,** 1194 (1973).
19. V. N. Korwar, Ph.D. Thesis, California Institute of Technology, Pasadena (1980).
20. J. W. Goodman, Proc. IEEE **53,** 1688 (1965).
21. W. J. Dixon and F. J. Massey, *Introduction to Statistical Analysis* (McGraw-Hill, New York, 1969).
22. B. D. Guenther, C. R. Christensen, and A. Jain, at IEEE Computer Society Conference on Pattern Recognition and Image Processing, 78CH1318-5C (1978).

Meetings Calendar *continued from page 319*

1981

May

11–15 15th Int. Symp. Remote Sensing of Environment, Ann Arbor *Remote Sensing Ctr., Environmental Res. Inst. Mich., P.O. Box 8618, Ann Arbor, Mich. 48107*

17–23 Mariculture: Culture of Marine Invertebrates for Research Purposes course, Woods Hole, Mass. *Marine Biological Lab., Woods Hole, Mass. 02543*

June

? Am. Astronomical Soc. Mtg., Calgary *L. W. Frederick, Box 3818, University Station, Charlottesville, Va. 22903*

1–4 Laser 81—5th Int. Cong. & Int. Exhibition, Munich *Kallman Assoc., 30 Journal Sq., Jersey City, N.J. 07306*

7–10 5th Rare Earth-Cobalt Magnet Workshop, Roanoke, Va. *K. Strnat, Magnetics Lab. KL-365, U. Dayton, Dayton, Ohio 45469*

7–12 8th Canadian Congress of Applied Mechanics, Moncton, Canada *N. Srivastava, Faculty of Sci. & Eng., U. Moncton, Moncton, N.B., EIA 3E9.*

8–12 Int. Conf. Fourier Transform Infrared Spectroscopy, S. Carolina U. *J. Lephardt, Philip Morris R&D, P.O. Box 26583, Richmond, Va. 23261*

8–12 2nd Int. Conf. Precision Measurement and Fundamental Constants, NBS, Gaithersburg *B. Taylor, B-258, Metrology Bldg., NBS, Wash., D.C. 20234*

10–12 **Lasers and Electrooptics Conf.,** Wash., D.C. *OSA, 1816 Jefferson Pl. N.W., Wash., D.C. 20036*

15–19 Int. Joint Conf. Thermophysical Properties, NBS, Gaithersburg *A. Cezairliyan, Rm. 124, Hazards Bldg., NBS, Wash., D.C. 20234*

15–29 NATO Adv. Study Inst., Collective Excitations in Solids, Erice, Italy *P. DiBartola, Phys. Dept., Boston Coll., Chestnut Hill, Mass. 02167*

22–25 2nd Int. Mtg. Photoacoustic Spectroscopy, Berkeley *OSA, 1816 Jefferson Pl. N.W., Wash., D.C. 20036*

July

? Int. Conf. Luminescence, West Berlin *AIP, 335 E. 45 St., N. Y., N.Y. 10017*

7–10 3rd Int. Conf. Hot Carriers in Semiconductors, Montpelier, France *J. Nougier, U. Sciences et Techniques de Languedoc, Centre d'Etudes d'Electronique des Solides, 34060 Montpellier Cedex, France*

14–18 15th Int. Conf. Phenomena in Ionized Gases, Minsk. *Organizing Comm. of ICPIG-15, Inst. of Phys., BSSR Academy of Sci., Leninskii Prospect, 70, Minsk, BSSR 220602, U.S.S.R.*

continued on page 329